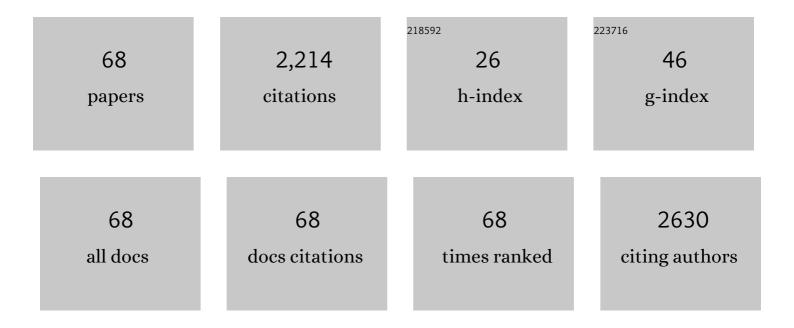
Wilson K S Chiu

List of Publications by Year in descending order

Source: https://exaly.com/author-pdf/1150162/publications.pdf Version: 2024-02-01



#	Article	IF	CITATIONS
1	Mono- and Multi-Objective CFD Optimization of Graded Foam-Filled Channels. Materials, 2022, 15, 968.	1.3	19
2	<i>In Situ</i> Determination of Speciation and Local Structure of NaCl–SrCl ₂ and LiF–ZrF ₄ Molten Salts. Journal of Physical Chemistry B, 2022, 126, 1539-1550.	1.2	5
3	Three-dimensional imaging of grain boundaries via quantitative fluorescence X-ray tomography analysis. Communications Materials, 2022, 3, .	2.9	5
4	Stability & Kinetics of the Bipolar Membrane Interface: Implications for Electrochemical Technologies. Journal of the Electrochemical Society, 2020, 167, 164513.	1.3	9
5	Anion Exchange Membrane Fuel Cell Performance in the Presence of Carbon Dioxide: An Investigation into the Self-Purging Mechanism. Journal of the Electrochemical Society, 2019, 166, F810-F820.	1.3	14
6	Predicting the Effects of Carbon Dioxide on the Conductivity of Electrospun Anion Exchange Membranes. Journal of the Electrochemical Society, 2019, 166, F1047-F1054.	1.3	4
7	Professor Yogesh Jaluria on his 70th Birthday. International Journal of Heat and Mass Transfer, 2019, 140, 1106-1107.	2.5	0
8	Simultaneous threeâ€dimensional elemental mapping of Hollandite and Pyrochlore material phases in ceramic waste form materials. Journal of the American Ceramic Society, 2019, 102, 5620-5631.	1.9	0
9	Multimodal hard x-ray imaging with resolution approaching 10 nm for studies in material science. Nano Futures, 2018, 2, 011001.	1.0	89
10	Anion Exchange Membrane Ionic Conductivity in the Presence of Carbon Dioxide under Fuel Cell Operating Conditions. Journal of the Electrochemical Society, 2017, 164, F1063-F1073.	1.3	14
11	Evolution of 3-D Transport Pathways and Triple-Phase Boundaries in the Ni-YSZ Hydrogen Electrode upon Fuel Cell or Electrolysis Cell Operation. ECS Transactions, 2017, 78, 3205-3215.	0.3	9
12	Threeâ€dimensional mapping of crystalline ceramic waste form materials. Journal of the American Ceramic Society, 2017, 100, 3722-3735.	1.9	6
13	Analytical transport network theory to guide the design of 3-D microstructural networks in energy materials: Part 1. Flow without reactions. Journal of Power Sources, 2017, 372, 297-311.	4.0	4
14	Analytical transport network theory to guide the design of 3-D microstructural networks in energy materials: Part 2. Flow with reactions. Journal of Power Sources, 2017, 372, 312-324.	4.0	3
15	Lord Kelvin and Weaire–Phelan Foam Models: Heat Transfer and Pressure Drop. Journal of Heat Transfer, 2016, 138, .	1.2	66
16	<i>In Situ</i> Heater Design for Nanoscale Synchrotron-Based Full-Field Transmission X-Ray Microscopy. Microscopy and Microanalysis, 2015, 21, 290-297.	0.2	5
17	Transient ion exchange of anion exchange membranes exposed to carbon dioxide. Journal of Power Sources, 2015, 296, 225-236.	4.0	27
18	Extension of anisotropic effective medium theory to account for an arbitrary number of inclusion types. Journal of Applied Physics, 2015, 117, .	1.1	79

WILSON K S CHIU

#	Article	IF	CITATIONS
19	Numerical Analysis of Heat Transfer and Pressure Drop in Metal Foams for Different Morphological Models. Journal of Heat Transfer, 2014, 136, .	1.2	58
20	Effect of orientation anisotropy on calculating effective electrical conductivities. Journal of Applied Physics, 2014, 115, 203503.	1.1	8
21	A rapid analytical assessment tool for three dimensional electrode microstructural networks with geometric sensitivity. Journal of Power Sources, 2014, 246, 322-334.	4.0	27
22	Characterization of 3D interconnected microstructural network in mixed ionic and electronic conducting ceramic composites. Nanoscale, 2014, 6, 4480.	2.8	19
23	Analytical solutions for extended surface electrochemical fin models. Journal of Power Sources, 2014, 265, 282-290.	4.0	9
24	Three-Dimensional Microstructural Imaging of Sulfur Poisoning-Induced Degradation in a Ni-YSZ Anode of Solid Oxide Fuel Cells. Scientific Reports, 2014, 4, 5246.	1.6	33
25	Three-dimensional microstructural imaging methods for energy materials. Physical Chemistry Chemical Physics, 2013, 15, 16377.	1.3	72
26	Multiphysics Design and Development of Heterogeneous Functional Materials for Renewable Energy Devices: The HeteroFoaM Story. Journal of the Electrochemical Society, 2013, 160, F470-F481.	1.3	12
27	Carbonate and Bicarbonate Ion Transport in Alkaline Anion Exchange Membranes. Journal of the Electrochemical Society, 2013, 160, F994-F999.	1.3	67
28	<i>In-situ</i> observation of nickel oxidation using synchrotron based full-field transmission X-ray microscopy. Applied Physics Letters, 2013, 102, .	1.5	14
29	Quantitative x-ray phase imaging at the nanoscale by multilayer Laue lenses. Scientific Reports, 2013, 3, 1307.	1.6	48
30	Microstructural Effects on Electronic Charge Transfer in Li-Ion Battery Cathodes. Journal of the Electrochemical Society, 2012, 159, A598-A603.	1.3	18
31	Focused ion beam preparation of samples for X-ray nanotomography. Journal of Synchrotron Radiation, 2012, 19, 789-796.	1.0	31
32	Zone-doubled Fresnel zone plates for high-resolution hard X-ray full-field transmission microscopy. Journal of Synchrotron Radiation, 2012, 19, 705-709.	1.0	59
33	High CO2 permeation flux enabled by highly interconnected three-dimensional ionic channels in selective CO2 separation membranes. Energy and Environmental Science, 2012, 5, 8310.	15.6	124
34	Nondestructive volumetric 3-D chemical mapping of nickel-sulfur compounds at the nanoscale. Nanoscale, 2012, 4, 1557.	2.8	12
35	Species transport in a high-pressure oxygen-generating proton-exchange membrane electrolyzer. International Journal of Hydrogen Energy, 2012, 37, 12451-12463.	3.8	10
36	Oxidation states study of nickel in solid oxide fuel cell anode using x-ray full-field spectroscopic nano-tomography. Applied Physics Letters, 2012, 101, .	1.5	21

WILSON K S CHIU

#	Article	IF	CITATIONS
37	Three-dimensional microstructural changes in the Ni–YSZ solid oxide fuel cell anode during operation. Acta Materialia, 2012, 60, 3491-3500.	3.8	93
38	Reactor scale modeling of multi-walled carbon nanotube growth. Applied Surface Science, 2011, 257, 5931-5937.	3.1	3
39	Analytical investigations of varying cross section microstructures on charge transfer in solid oxide fuel cell electrodes. Journal of Power Sources, 2011, 196, 4695-4704.	4.0	28
40	Three-dimensional mapping of nickel oxidation states using full field x-ray absorption near edge structure nanotomography. Applied Physics Letters, 2011, 98, .	1.5	60
41	Special Issue on Advanced Thermal Processing. Journal of Heat Transfer, 2011, 133, .	1.2	1
42	Direct Internal Reformation and Mass Transport in the Solid Oxide Fuel Cell Anode: A Poreâ€scale Lattice Boltzmann Study with Detailed Reaction Kinetics. Fuel Cells, 2010, 10, 1143-1156.	1.5	14
43	Pore-scale investigation of mass transport and electrochemistry in a solid oxide fuel cell anode. Journal of Power Sources, 2010, 195, 2331-2345.	4.0	44
44	Ionic Equilibrium and Transport in the Alkaline Anion Exchange Membrane. Journal of the Electrochemical Society, 2010, 157, B1024.	1.3	37
45	A Dusty Fluid Model for Predicting Hydroxyl Anion Conductivity in Alkaline Anion Exchange Membranes. Journal of the Electrochemical Society, 2010, 157, B327.	1.3	157
46	Nondestructive Nanoscale 3D Elemental Mapping and Analysis of a Solid Oxide Fuel Cell Anode. Journal of the Electrochemical Society, 2010, 157, B783.	1.3	116
47	Non invasive, multiscale 3D X-Ray characterization of porous functional composites and membranes, with resolution from MM to sub 50 NM. Journal of Physics: Conference Series, 2009, 152, 012059.	0.3	19
48	Boundary integral method for the evolution of slender viscous fibres containing holes in the cross-section. Journal of Fluid Mechanics, 2009, 621, 155-182.	1.4	6
49	Modeling of gas transport through a tubular solid oxide fuel cell and the porous anode layer. Journal of Power Sources, 2008, 176, 200-206.	4.0	26
50	Nondestructive Reconstruction and Analysis of SOFC Anodes Using X-ray Computed Tomography at Sub-50â€,nm Resolution. Journal of the Electrochemical Society, 2008, 155, B504.	1.3	186
51	Thermal Radiative Properties of a Semitransparent Fiber Coated With a Thin Absorbing Film. Journal of Heat Transfer, 2007, 129, 763-767.	1.2	5
52	Lattice Boltzmann modeling of 2D gas transport in a solid oxide fuel cell anode. Journal of Power Sources, 2007, 164, 631-638.	4.0	102
53	Growth kinetics and microstructure of carbon nanotubes using open air laser chemical vapor deposition. Diamond and Related Materials, 2006, 15, 1438-1446.	1.8	3
54	Heat and Mass Transfer in a CVD Optical Fiber Coating Process by Propane Precursor Gas. Numerical Heat Transfer; Part A: Applications, 2006, 50, 147-163.	1.2	2

WILSON K S CHIU

#	Article	IF	CITATIONS
55	Application of an Anode Model to Investigate Physical Parameters in an Internal Reforming Solid-Oxide Fuel Cell. Journal of Fuel Cell Science and Technology, 2005, 2, 136-140.	0.8	8
56	Growth kinetics and microstructure of carbon deposited on quartz plates and optical fibers by open-air laser-induced chemical vapor deposition. Thin Solid Films, 2005, 492, 79-87.	0.8	2
57	Hybrid Method to Calculate Direct Exchange Areas Using the Finite Volume Method and Midpoint Intergration. Journal of Heat Transfer, 2005, 127, 911-917.	1.2	6
58	A TWO-DIMENSIONAL SCHEME FOR AXISYMMETRIC RADIATIVE HEAT TRANSFER USING THE FINITE-VOLUME METHOD. Numerical Heat Transfer, Part B: Fundamentals, 2005, 47, 199-211.	0.6	17
59	Temperature prediction for CO2 laser heating of moving glass rods. Optics and Laser Technology, 2004, 36, 131-137.	2.2	30
60	Microstructural characterization of thin carbon films deposited from hydrocarbon mixtures. Surface and Coatings Technology, 2004, 182, 131-137.	2.2	17
61	Open-air carbon coatings on fused quartz by laser-induced chemical vapor deposition. Carbon, 2003, 41, 673-680.	5.4	36
62	Heat treatment of thin carbon films and the effect on residual stress, modulus, thermal expansion and microstructure. Carbon, 2003, 41, 1867-1875.	5.4	25
63	Laser-induced carbon CVD on a moving fused quartz substrate: morphological and oscillatory deposition characteristics. Carbon, 2003, 41, 2307-2316.	5.4	2
64	Characterization of CVD carbon films for hermetic optical fiber coatings. Surface and Coatings Technology, 2003, 168, 1-11.	2.2	47
65	Residual stress measurement in thin carbon films by Raman spectroscopy and nanoindentation. Thin Solid Films, 2003, 429, 190-200.	0.8	75
66	TEMPERATURE DISTRIBUTION OF AN OPTICAL FIBER TRAVERSING THROUGH A CHEMICAL VAPOR DEPOSITION REACTOR. Numerical Heat Transfer; Part A: Applications, 2003, 43, 221-237.	1.2	33
67	Calculation of Direct Exchange Areas for Nonuniform Zones Using a Reduced Integration Scheme. Journal of Heat Transfer, 2003, 125, 839-844.	1.2	14
68	Modeling Metallic Halide Local Structures in Salt Melts Using a Genetic Algorithm. Journal of Physical Chemistry C, 0, , .	1.5	0